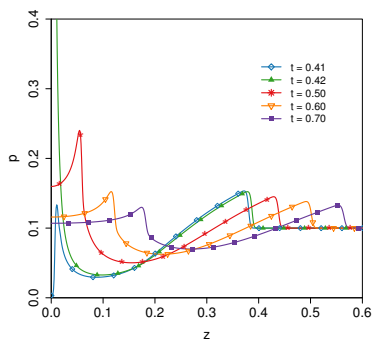
Lattice Boltzmann models for relativistic shocks



arXiv:1612.01287

Robert Blaga, Victor E. Ambruș

DSFD 2017 10-14 July, Erlangen, Germany

Overview

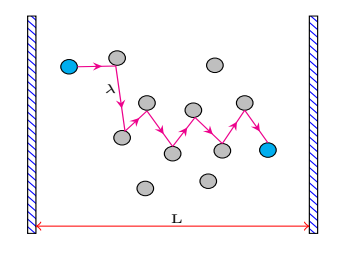
- What is this Boltzmann?
 - Of fluids and gases
 - The equation
 - Transport coefficients
- 2 Relativistic Lattice Boltzmann
 - Lattice Boltzmann model
- 3 Applications
 - Harmonic perturbation
 - Cartesian Sod problem
 - Spherical Sod problem

Of fluids and gases

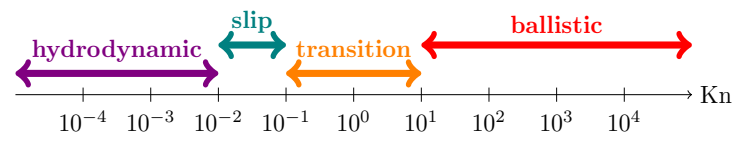
Fluid: physical system with large number of (interacting) constituents

Levels of description:

- macroscopic: hydrodynamics/Navier-Stokes eqs.
- mesoscopic: kinetic theory/Boltzmann eq.
- microscopic: molecular dynamics/Newton's eqs.



$$\mathsf{Kn} = \lambda/\mathsf{L}$$
.



The equation

• Relativistic Boltzmann equation:

$$\left(p^{\hat{\mu}}\partial_{\hat{\mu}} - \Gamma^{\hat{i}}_{\hat{\mu}\hat{\nu}}p^{\hat{\mu}}p^{\hat{\nu}}\partial_{p^{\hat{i}}}\right)f(t,\vec{x},\vec{p}) = C[f] \tag{1}$$

Anderson-Witting collision operator:

$$C[f] = \frac{u^{\hat{\alpha}} p_{\hat{\alpha}}}{\tau} \left(f - f^{(eq)} \right) \tag{2}$$

Maxwell-Jüttner distribution:

$$f^{(eq)} = \frac{n}{8\pi T^3} \exp\left(\frac{u^{\hat{\alpha}} p_{\hat{\alpha}}}{T}\right),\tag{3}$$

with the mass-shell conditions: $p^{\mu}p_{\mu}=0$, for ultra-relativistic particles.

Macroscopic profiles

Macroscopic fields are defined as moments of the distribution function.

Particle four-flow:

$$N^{\hat{\alpha}} = \int \frac{d^3p}{p^{\hat{t}}} f \, p^{\hat{\alpha}} \tag{4}$$

Energy-momentum tensor:

$$T^{\hat{\alpha}\hat{\beta}} = \int \frac{d^3p}{p^{\hat{\epsilon}}} f \, p^{\hat{\alpha}} p^{\hat{\beta}} \tag{5}$$

Higher order moments:

$$T^{\hat{\alpha}...\hat{\omega}} = \int \frac{d^3p}{p^{\hat{t}}} f p^{\hat{\alpha}}...p^{\hat{\omega}}$$
 (6)

Transport coefficients

The particle 4-flow and energy-momentum tensor of a fluid of ultra-relativisitic particles, in the Landau frame:

$$N^{\mu} = nu^{\mu} - \frac{n}{(E+P)}q^{\mu}, \qquad T^{\mu\nu} = (E+P)u^{\mu}u^{\nu} + P\eta^{\mu\nu} + \Pi^{\mu\nu}, \tag{7}$$

together with the ultra-relativistic equations of state: P = E/3 = nT.

For a system which is homogeneous along the ${\sf x}$ and ${\sf y}$ axis, the heat-flux and shear-stress have the form:

In five-field theory, the heat-flux and shear pressure are related to the gradients of the pressure, temperature, and velocity, as follows:

$$\begin{array}{lcl} q^{\mu} & = & q(\beta,0,0,1) \\ \Pi^{\mu\nu} & = & \Pi \begin{pmatrix} \beta^2 \gamma^2 & 0 & 0 & \beta \gamma^2 \\ 0 & -\frac{1}{2} & 0 & 0 \\ 0 & 0 & -\frac{1}{2} & 0 \\ \beta \gamma^2 & 0 & 0 & \gamma^2 \end{pmatrix} \end{array}$$

$$q = \frac{\lambda T \gamma^2}{4t} (1 - \beta \xi) \partial_{\xi} \ln \left(\frac{P}{T^4} \right)$$
 (8)

$$\Pi = -\frac{4\eta}{3t}(1-\beta\xi)\partial_{\xi}(\gamma\beta), \qquad (9)$$

where $\xi = \frac{x}{t}$ the self-similarity variable.

	Chapman-Enskog (CE)	Grad's method (G)
λ - heat conductivity	$4/3 \text{ n}\tau$	$4/5 \; \mathrm{n} au$
η - shear viscosity	4/5 Pτ	2/3 Pτ

Lattice Boltzmann model

We project the equilibrium distribution function onto complete sets of orthogonal polynomials, with respect each momentum-space coordinates¹:

$$f^{(eq)}(t, \vec{x}, \vec{p}) = \frac{e^{-p/T_0}}{T_0^3} \sum_{\ell=0}^{N_L} \sum_{s=0}^{N_{\Omega}} a_{\ell,s}^{(eq)}(\vec{x}, t) P_s(\xi) L_{\ell}^{(2)}(p/T_0)$$
 (10)

② The second ingredient is the discretisation of the momentum space. For massless particles we have $p^{\hat{t}} = |\vec{p}| \equiv p$ and $v^{\hat{\alpha}} = p^{\hat{\alpha}}/p$. We convert the integrals in the particle four-flow and energy momentum tensor into finite sums, as follows^{2,3}

$$\begin{split} N^{\hat{\alpha}} &= \int\limits_{0}^{\infty} dp \, p^{2} \int\limits_{-1}^{1} d\xi \int\limits_{0}^{2\pi} d\varphi \, f \, v^{\hat{\alpha}} &= \sum_{a=1}^{Q_{L}} \sum_{b=1}^{Q_{\xi}} \sum_{c=1}^{Q_{\varphi}} f_{abc} \, v_{bc}^{\hat{\alpha}}, \\ T^{\hat{\alpha}\hat{\beta}} &= \int\limits_{0}^{\infty} dp \, p^{3} \int\limits_{-1}^{1} d\xi \int\limits_{0}^{2\pi} d\varphi \, f \, v^{\hat{\alpha}} v^{\hat{\beta}} = \sum_{a=1}^{Q_{L}} \sum_{b=1}^{Q_{\xi}} \sum_{c=1}^{Q_{\varphi}} f_{abc} \, p_{a} v_{bc}^{\hat{\alpha}} v_{bc}^{\hat{\beta}}, \\ f_{abc} &= \frac{2\pi w_{a}^{L} w_{b}^{\xi}}{Q_{\varphi} \, e^{-p_{a}/T_{0}}/T_{0}^{3}} \, f(p_{a}, \xi_{b}, \varphi_{c}). \end{split}$$

Numerical scheme: WENO 5 + TVD-RK3



(11)

We have introduced spherical coordinates in the momentum space: $\vec{p} = (p, \theta, \phi)$, with the notation $\xi = \cos \theta$.

²V.E. Ambruş and V. Sofonea, *Phys. Rev. E* **86** (2012).

³R. Blaga and V.E. Ambruş, preprint arXiv:1612.01287 (2016).

Harmonic perturbation

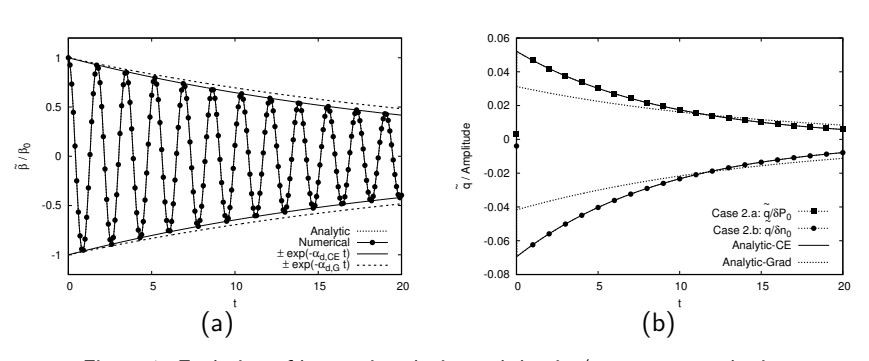


Figure 1: Evolution of harmonic velocity and density/pressure perturbation.

Note: The results match the analytic solution, with the transport coefficients obtained through the Chapman-Enskog method.^{4,5,6}

⁴V. E. Ambrus. arXiv:1706.05310, (2017).

⁵A. Gabbana, M. Mendoza, S. Succi, and R. Tripiccione. arXiv:1704.02523, (2017).

⁶ A. Jaiswal. Phys. Rev. C **87**, (2013).

Cartesian Sod problem - hydrodynamic regime

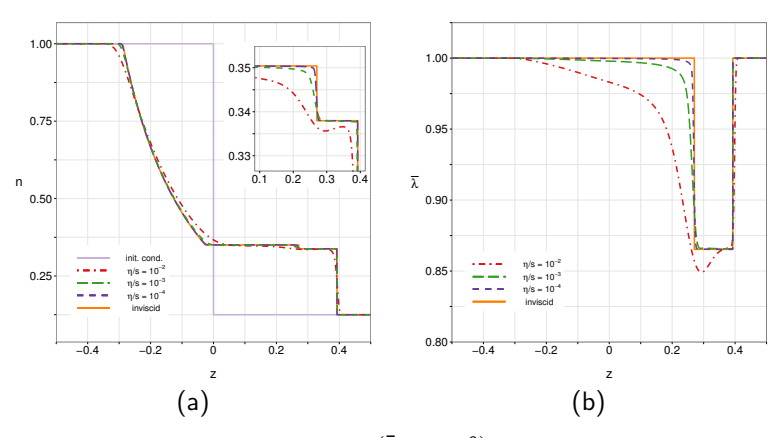


Figure 2: (a) Density profile and (b) fugacity $(\bar{\lambda} = n/T^3)$ of the fluid in the Cartesian Sod-shock tube problem, at different relaxation times.⁷

Number of velocities: $N_{\text{vel}} = Q_L \times Q_{\xi} \times Q_{\phi} = 2 \times 4 \times 1 = 8.$ (12)

⁷L. Rezzolla and O. Zanotti. Relativistic hydrodynamics. Oxford University Press, (2013) → ⟨ ≧ ⟩ ⟨ ≧ ⟩ ⟨ ≧ ⟩ ⟨

Cartesian Sod problem - hydrodynamic regime

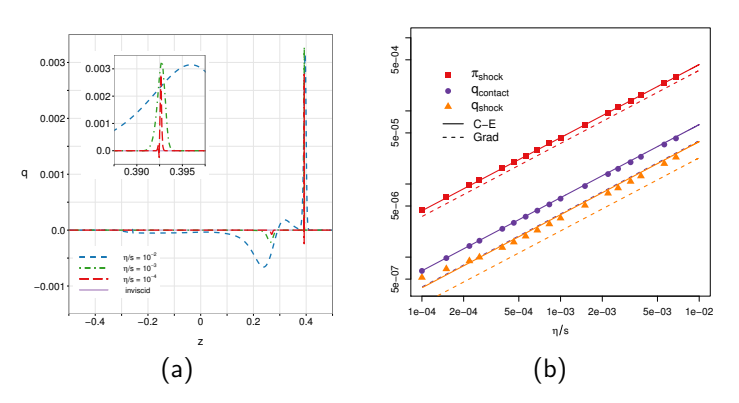


Figure 3: a) Heat flux in the Cartesian Sod problem, at different relaxation times. b) Integrated values of the heat-flux and shear-stress around the shock front and contact discontinuity.

Heat-flux at the contact:
$$\int_{z_{C}-\delta z}^{z_{C}+\delta z} q \, dz = \frac{1}{8} (\lambda_{I} T_{I} + \lambda_{II} T_{II}) \ln \left(\frac{P_{II}}{T_{II}^{4}} \frac{T_{I}^{4}}{P_{I}} \right). \tag{13}$$

Cartesian Sod problem - viscous regime

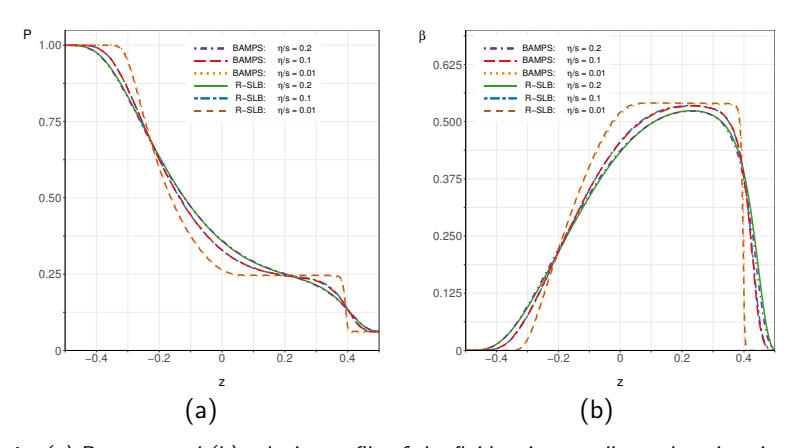


Figure 4: (a) Pressure and (b) velocity profile of the fluid at intermediate relaxation times, as compared to the BAMPS results reported in Bouras, et.al. (2009).⁸

Relation to relaxation time:
$$\tau = \frac{\eta}{s} \frac{5}{T} \left[1 - \frac{1}{4} \ln \left(\frac{n}{T^3} \right) \right]$$
 (14)

⁸ Bouras, E. Molnar, H. Niemi, Z. Xu, A. El, O. Fochler, C. Greiner, and D. Rischke. Phys Rev. Lett. 103, (2009).

Cartesian Sod problem - ballistic regime

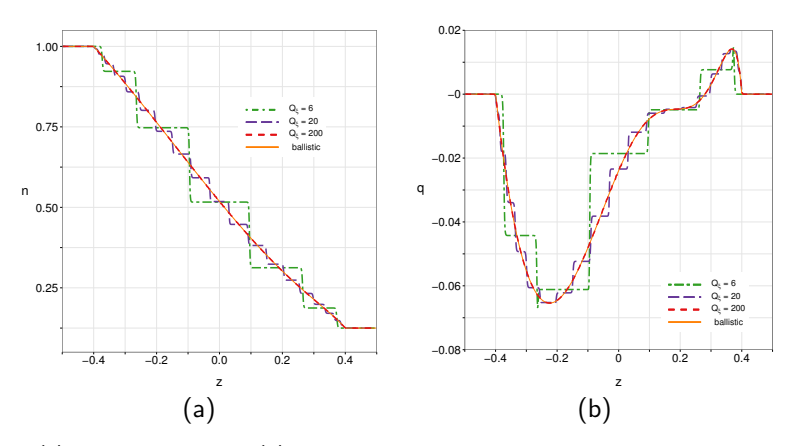


Figure 5: (a) Density profile and (b) heat-flux in the ballistic regime. A large velocity set is needed to obtain good agreement with the analytical solution.

Number of velocities: $N_{vel} = Q_L \times Q_{\xi} \times Q_{\phi} = 2 \times 200 \times 1 = 400.$ (15)

Spherical Sod problem - hydrodynamic regime

Boltzmann eq. in spherical coordinates:

$$\partial_t f + \frac{\xi}{r^2} \partial_r (r^2 f) + \frac{1}{r} \frac{\partial}{\partial \xi} [(1 - \xi^2) f] = -\frac{1}{\tau} \left(u^{\hat{t}} - \xi u^z \right) (f - f^{(eq)}), \qquad \xi = \cos \theta \qquad (16)$$

 The problems arising from the divergence at the origin are resolved by employing the following scheme¹⁰:

$$\frac{\xi}{r^2} \frac{\partial (r^2 f)}{\partial r} = \frac{\xi}{r^2} \frac{\partial r^3}{\partial r} \frac{\partial (f r^2)}{\partial r^3}
= 3 \frac{r_{s+1/2}^2 \mathcal{F}_{s+1/2} - r_{s-1/2}^2 \mathcal{F}_{s-1/2}}{r_{s-1/2}^3 - r_{s-1/2}^3}$$

• The fluxes $\mathcal{F}_{s\pm 1/2}$ are obtained with the WENO 5 procedure.

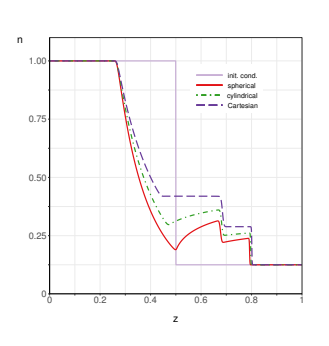


Figure 6: Density profile of the fluid in Sod problem setup for planar, cylindrical and spherical geometry.⁹

⁹ Martí, J.M., et al., Astrophys. J **479**, (1997).

T.P. Downes, P. Duffy, and S.S. Komissarov., Mon. Not. R. Astron. Soc. 332 (2002): 🗇 🔻 📜 🕨 👢

Spherical Sod problem - hydrodynamic regime

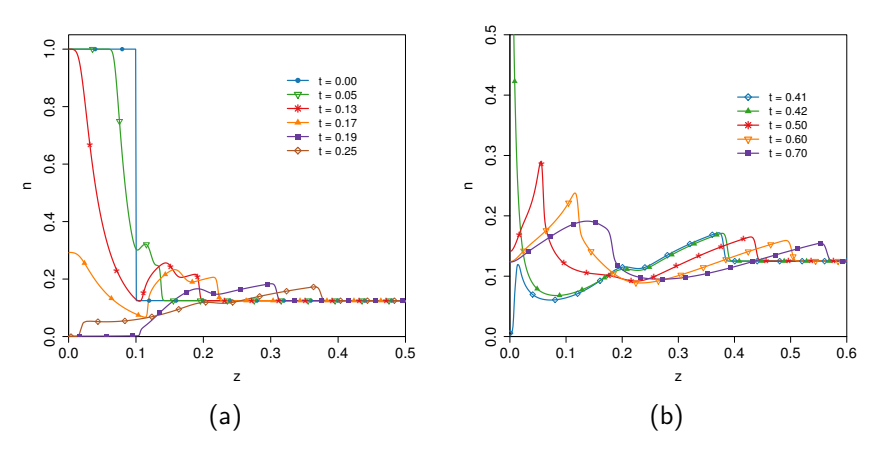


Figure 7: Density profile of the spherical Sod problem at (a) small and (b) large times. After the rarefaction wave reaches the origin the pressure drops several orders of magnitude. The negative pressure gradient accelerates the fluid back towards the origin, producing a high velocity secondary shock. As the second shock reaches the origin, a very high density spike forms, which then propagates outwards.

Spherical Sod problem - hydrodynamic regime

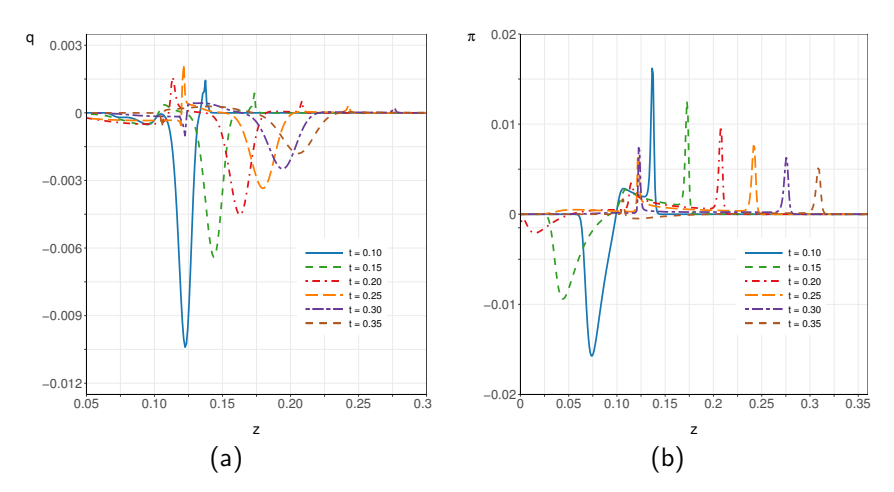


Figure 8: (a) Heat-flux and (b) shear pressure of the fluid in spherical Sod problem, at various instances of time.

Spherical Sod problem - ballistic regime

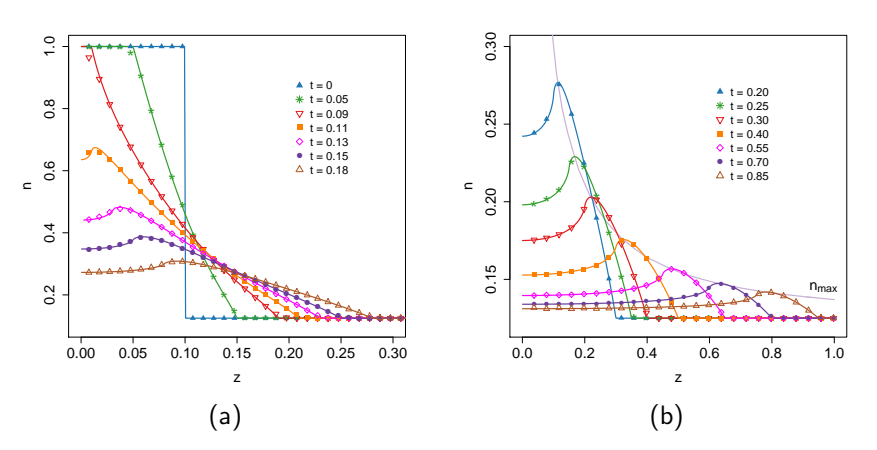


Figure 9: Density profile of the fluid in the cylindrical Sod problem, in the ballistic regime. Panel (a) shows instances of time around the moment when the rarefaction wave arrives at the origin, while panel (b) shows larger times, when a shell of high density fluid propagates outwards.

Conclusion

- We have developed lattice Boltzmann models, based on Gauss quadratures, adapted for problems with planar, cylindrical and spherical geometries
- The models have been tested on various problems with very good agreement compared to the analytical solutions and other results reported in the literature, across the whole spectrum of the relaxation time
- Possible areas of future extension and application:
 - ⇒ the physics of quark-gluon plasma
 - ⇒ astrophysical flows
 - \Rightarrow condensed matter (electrons in metals, graphene, and so on)

Acknowledgement

Thank you!

This work was supported by a grant from the Romanian National Authority for Scientific Research and Innovation, CNCS-UEFISCDI, project number PN-II-RU-TE-2014-4-2910.